

## Internal Mechanical Response of a Polymer in Solution

Adam E. Cohen and W. E. Moerner

*Departments of Physics and Chemistry, Stanford University, Stanford, California 94305, USA\**

(Received 19 September 2006; published 14 March 2007)

We observed single molecules of fluorescently labeled double-stranded (ds)  $\lambda$  DNA held in an anti-Brownian electrokinetic trap. From the measured density fluctuations we extract the density-density response function of the molecule over times  $>4.5$  ms and distances  $>250$  nm, i.e., how a perturbation in density in one part of the molecule propagates through the rest of the molecule. We find a nonmonotonic radial dependence of the relaxation time. In contrast with earlier measurements on freely diffusing dsDNA, we observe clear signs of internal hydrodynamic interactions.

DOI: [10.1103/PhysRevLett.98.116001](https://doi.org/10.1103/PhysRevLett.98.116001)

PACS numbers: 83.10.Mj, 87.14.Gg, 87.15.Tt, 87.15.Ya

Thermal fluctuations agitate molecules in solution over a broad range of times and distances. By passively watching the shape fluctuations of a thermally driven biopolymer, one can infer properties of the underlying interactions that determine the motion.

Dynamic light scattering (DLS) and fluorescence correlation spectroscopy (FCS) each probe specific low-dimensional correlation functions of the shape fluctuations; these can be compared to predictions of Rouse, Zimm, or other hydrodynamic models [1]. The two techniques are complementary in that DLS probes fluctuations at a fixed  $k$  vector and FCS at a fixed position vector. Both techniques are also limited in the time scales they can probe: very fast fluctuations occur over distances too short to be detected optically, and very slow fluctuations are masked by translational diffusion.

DLS has been used to measure the few longest relaxation times of DNA, and much theory has been devoted to predicting scattering functions for different polymer models [2,3]. FCS has also been used to probe the dynamic fluctuations of fluorescently labeled DNA [4,5]. Recently Shusterman and co-workers [6] probed the dynamics of the end monomer in single-stranded (ss) and double-stranded (ds) DNA using FCS. They observed Zimm dynamics in the ssDNA, but, surprisingly, Rouse dynamics in the dsDNA on time scales  $<10$  ms. In contrast, the translational diffusion of dsDNA obeys Zimm scaling to high accuracy [7]. Shusterman *et al.* argued that a semiflexible partially draining polymer should show Rouse dynamics on short time scales and Zimm dynamics on long time scales. However, the observation times required to detect Zimm dynamics in dsDNA are longer than can be achieved with FCS.

Here we directly measure the underlying time-dependent conformations of individual dsDNA molecules over times  $>4.5$  ms and distances  $>250$  nm. FCS-like and DLS-like correlation functions are special cases of the density-density covariance obtained from our data. Our experiment lacks the short-time resolution of DLS and FCS, but probes long-time dynamics (milliseconds to sec-

onds) that are masked by translational diffusion in the other techniques. The data presented here provide the first detailed *spatial* picture of the fluctuating dynamics within a single conformationally relaxed polymer molecule.

To study a single molecule in equilibrium, one would like to eliminate the motion of the center of mass (c.m.), without affecting internal motions. We used an anti-Brownian electrokinetic (ABEL) trap to achieve this. The apparatus has been described previously and is capable of trapping individual large protein molecules in solution [8].

Double-stranded  $\lambda$  DNA was fluorescently labeled and loaded into the ABEL trap. Experimental conditions are given in [9]. The  $\lambda$  DNA had a persistence length of  $l_p \approx 60$  nm, a contour length of  $L \approx 20 \mu\text{m}$ , and a radius of gyration  $R_G \approx 700$  nm. Molecules were held in the ABEL trap and a two-dimensional projection of their conformational motions was recorded with video microscopy at 4.5 ms/frame. Twenty-one separate molecules were trapped (yielding between 2000 and 4000 images/molecule; total data set 58 421 frames; Fig. 1). The molecules were labeled with a uniform density of fluorophores, so the fluorescence intensity at each point in an image was proportional to the density of DNA averaged over the point-spread function of the microscope at a corresponding point in the sample [9]. A trapped molecule undergoes small fluctuations about the trap center; for the purposes of analyzing the internal dynamics we translated each image to keep the c.m. fixed. We also normalized the intensity in each image to account for the slow rate of photobleaching during a measurement.

An important question is whether the trapping feedback fields affect the conformation of the DNA. To test for such



FIG. 1. Series of images showing shape fluctuations of fluorescently labeled  $\lambda$  DNA (here every eighth image from the full movie is shown). Scale bar  $2 \mu\text{m}$ .

interactions experimentally, we calculated the correlation between the applied voltage and the measured shape of the molecule, as follows. Let  $I(\mathbf{r}, t)$  be the intensity distribution (after removing motion of the c.m.). Let  $\langle I(\mathbf{r}, t) \rangle$  be the time-average distribution, and  $\delta I(\mathbf{r}, t) \equiv I(\mathbf{r}, t) - \langle I(\mathbf{r}, t) \rangle$  be the instantaneous deviation from this average. The feedback voltages are  $V_x$  and  $V_y$ . We found that  $\langle V_x(t_2)\delta I(\mathbf{r}, t_1) \rangle \approx 0$  and  $\langle V_y(t_2)\delta I(\mathbf{r}, t_1) \rangle \approx 0$  to within the experimental uncertainty, for all  $t_2$ ,  $t_1$ , and  $\mathbf{r}$ . Coupling between the feedback voltage and the conformation is thus small enough to be neglected here. This finding is consistent with the theoretical argument that electrokinetic force and drag act uniformly along the DNA backbone [10] and the experimental observation that the free-solution mobility of DNA is independent of contour length or conformation [11]. We cannot rule out the possibility that higher order effects modify the conformation to a small extent, but the present measurements are not sensitive to such perturbations. Finite element simulations show that the electric field is homogeneous to within  $<0.1\%$  over the size of the DNA molecule [12].

Another possible source of bias is the screening of long-range hydrodynamic interactions by the no-slip condition on the trap walls. Below we find that the c.m. diffusion coefficient  $D$  is 24% less than its free-solution value. When a polymer is confined,  $D$  decreases more rapidly than the internal relaxation rates. This difference arises because the hydrodynamic disturbance created by diffusion of the c.m. decays more slowly with distance than does the disturbance created by internal relaxation [13]. Thus we expect errors in the internal relaxation rates to be  $<24\%$ .

We first analyzed the time-averaged distribution of fluorescence intensity  $\langle I(\mathbf{r}) \rangle$  (and hence molecular density), keeping the c.m. fixed. Figure 2 shows that the density distribution has fat tails relative to a Gaussian. This non-Gaussian distribution has been predicted on the basis of a simple random walk model, as follows [14]. For a pure

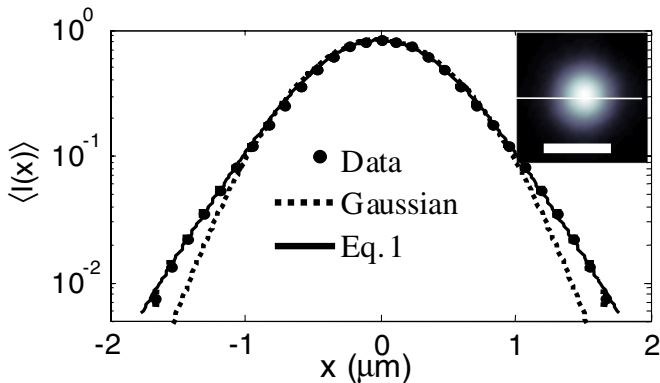


FIG. 2 (color online). Non-Gaussian distribution of mass about the c.m. of a random walk polymer. The fitting parameters are as follows: for the 1D Gaussian fit,  $R_G^2 = 0.48 \mu\text{m}^2$ ; for the fit to Eq. (1),  $R^2 = 1.37 \mu\text{m}^2$ . Inset: Image of the average density; white line indicates the cross section plotted in the main figure. Scale bar  $2 \mu\text{m}$ .

random walk polymer, each segment follows a Gaussian distribution about the c.m., but the width of this distribution is different for different segments: the ends wander further than the middle. The total density distribution is the sum of many Gaussians of distinct widths, and thus is not a Gaussian. This model predicts the density distribution  $\rho(\mathbf{r})$  to be

$$\rho(\mathbf{r}) = \frac{3}{2\pi R^2} \int_0^1 \frac{\exp(-3r^2/[2R^2(3\epsilon^2 - 3\epsilon + 1)])}{(3\epsilon^2 - 3\epsilon + 1)} d\epsilon, \quad (1)$$

where  $R^2$  is the mean-square end-to-end distance. As with a Gaussian, Eq. (1) has only one free parameter,  $R$ . Figure 2 shows that Eq. (1) is consistent with the data, implying that the average conformation is well-described by a simple non-self-avoiding random walk. Fisher showed that excluded volume (EV) interactions lead to a density distribution with *skinny* tails relative to a Gaussian [15], so we conclude that EV does not have a large effect on the *average shape* of  $\lambda$  DNA in our experiment.

Now we turn to the dynamics. The most general second-order measure of the internal dynamics is the density-density covariance

$$C(\mathbf{r}_1, \mathbf{r}_2, \tau) = \langle \delta I(\mathbf{r}_1, t)\delta I(\mathbf{r}_2, t + \tau) \rangle, \quad (2)$$

where  $\mathbf{r}_1$  and  $\mathbf{r}_2$  are measured relative to the c.m. and the average is taken over all  $t$ . Figure 3 shows one projection of  $C(\mathbf{r}_1, \mathbf{r}_2, \tau)$ .

The fluctuation-dissipation theorem relates the covariance  $C(\mathbf{r}_1, \mathbf{r}_2, \tau)$  to the linear mechanical response function of the molecule, i.e., how a coupling to the density at  $(\mathbf{r}_1, t)$  perturbs the density at some other place and time  $(\mathbf{r}_2, t + \tau)$  (at distances  $>250$  nm and lags  $>4.5$  ms). By observing the shape fluctuations we obtained this information without ever mechanically perturbing the molecule. Thermal fluctuations provide all possible sets of perturbations, and one merely has to filter the data to select the perturbation of interest. In biological systems, density perturbations may come from proteins that bind multiple DNA strands or from localized concentrations of condensing agents.

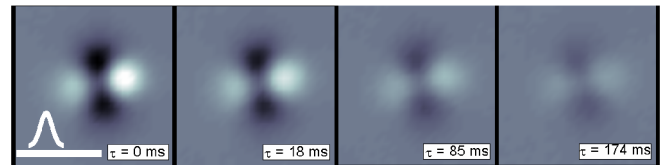


FIG. 3 (color online). Density-density covariance,  $C(\mathbf{r}_1, \mathbf{r}_2, \tau)$ , showing the decay of fluctuations within  $\lambda$  DNA. In these images  $\mathbf{r}_1$  is fixed 780 nm to the right of the c.m.. The lobed structure at  $\tau = 0$  is due to the requirement that the c.m. remain fixed: a fluctuation in density to the right is necessarily accompanied by a fluctuation of the same sign to the left. Scale bar  $2 \mu\text{m}$ ; white curve shows approximate point-spread function of the microscope.

The correlation functions probed by FCS and DLS are lower-dimensional projections of  $C(\mathbf{r}_1, \mathbf{r}_2, \tau)$ . In particular, the FCS spectrum is related to

$$G(\tau) = \sum_{\mathbf{R}} C(\mathbf{R}, \mathbf{R}, \tau), \quad (3)$$

and the DLS dynamic structure factor is related to

$$S(\mathbf{r}, \tau) = \sum_{\mathbf{R}} C(\mathbf{R} + \mathbf{r}, \mathbf{R}, \tau). \quad (4)$$

In both cases the correspondence is not exact because the quantities probed by FCS and DLS are dominated by diffusion of the c.m. at long times, while  $C(\mathbf{r}_1, \mathbf{r}_2, \tau)$  is not.

Figure 4(a) shows  $G(\tau)$  and a fit to a stretched exponential of the form  $G(\tau) \propto \exp[-(\tau/\tau_0)^\beta]$ , with a stretching exponent of  $\beta = 0.58 \pm 0.02$ . From de Gennes' models of dynamic light scattering, we expect a stretching exponent of  $\beta_{\text{Rouse}} = 1/2$  [16], and  $\beta_{\text{Zimm}} = 2/3$  [17]. The observed value of  $\beta$  indicates that hydrodynamic coupling is important on time scales of 10–500 ms, as predicted by Shusterman *et al.*, although hydrodynamic screening by the walls of the trap may reduce  $\beta$  from its free-solution value.

The dynamic structure factor provides a more detailed view of the dynamics by resolving the fluctuations into

spatial modes. When expressed in  $k$  space, we expect the long-time asymptotic behavior to obey  $S(\mathbf{k}, t) \propto \exp[-(t/\tau_k)^\beta]$  with  $\beta_{\text{Rouse}} = 1/2$  and  $\beta_{\text{Zimm}} = 2/3$  [1]. The time-dependence of  $S(\mathbf{k}, t)$  was fit to a stretched exponential, and Fig. 4(b) shows that the stretching exponent approaches the Rouse value of 1/2 for large  $k$  and the Zimm value of 2/3 for small  $k$ . As expected from the argument of Shusterman *et al.* applied to  $\lambda$  DNA, the transition occurs between  $k = 1$  and  $2 \mu\text{m}^{-1}$ . From this analysis of the internal fluctuations of ds  $\lambda$  DNA we conclude that the molecule exhibits both Rouse and Zimm behavior. Rouse behavior dominates at high wave vectors and Zimm at low wave vectors.

The quantities probed by DLS and FCS are both averaged over the entire molecule. This clearly discards information: the dynamics may be different in different parts of the molecule. To probe for such heterogeneity, we examined the position-dependent autocorrelation  $C(\mathbf{r}, \mathbf{r}, \tau)$ . This measure of polymer dynamics has not previously been studied either experimentally or theoretically. Interestingly, we find a nonmonotonic radial dependence in the decay of  $C(\mathbf{r}, \mathbf{r}, \tau)$ , with slowest decay near and far from the c.m., and considerably faster decay at intermediate radii [Fig. 4(c)]. This pattern is highlighted by examination of the radially averaged correlation times, calculated from the short-time rate of decay of  $C(\mathbf{r}, \mathbf{r}, \tau)$  [Fig. 4(d)].

Numerical simulations of a Rouse polymer in free solution also yielded an annular decay of  $C(\mathbf{r}, \mathbf{r}, \tau)$  [Fig. 4(d), solid line), indicating that this pattern is an intrinsic property of the polymer; not due to interactions with the walls of the trap or the feedback voltage. Details of the simulation are given in [9]. At present the physical origins of this nonmonotonic radial dependence are not clear, nor is it clear whether the difference between simulation and experiment at large  $r$  is due to wall interactions or to internal hydrodynamic interactions (both neglected in the simulations).

Finally, we analyze the small fluctuations of the c.m. about the trap center, and find a coupling between the internal degrees of freedom and the variance of the Brownian hops. This result is in contrast to both the Rouse and Zimm models, which allow no such coupling.

The technique of pseudofree trajectories uses the frame-by-frame measurements of center of brightness and the applied voltages to “undo” the effects of the feedback, yielding a random walk trajectory statistically similar to the one the particle would have followed had it not been trapped [8]. The hops in the pseudofree trajectories are  $\delta$  correlated [9] and yield an average diffusion coefficient  $D = 0.32 \pm 0.02 \mu\text{m}^2/\text{s}$ . This result is somewhat smaller than the value  $0.42 \pm 0.03 \mu\text{m}^2/\text{s}$  one would expect from the recent data of Robertson *et al.* [7], but the difference is consistent with a modest suppression due to hydrodynamic interactions with the walls of the trap [18].

Almost 40 years ago Dubois-Violette and de Gennes predicted that internal hydrodynamic interactions should

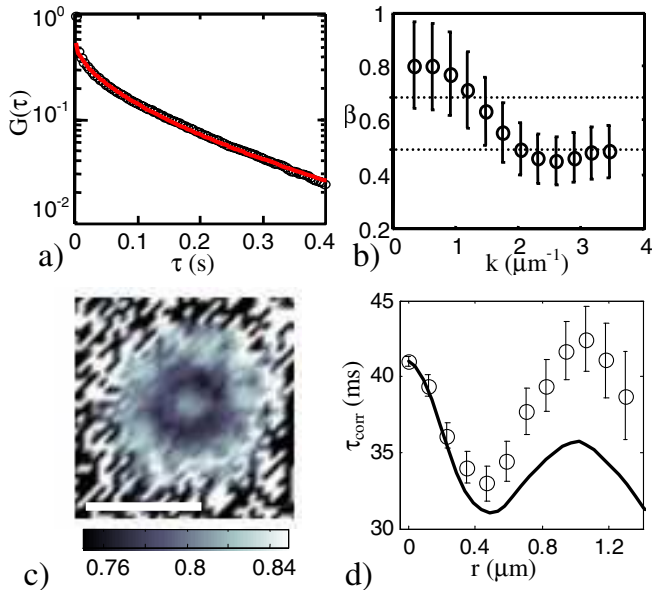


FIG. 4 (color online). Correlation functions of shape fluctuations. (a) Two-time correlation of the global shape fluctuations,  $G(\tau)$ , (circles), and fit to a stretched exponential (line). The  $\tau = 0$  term was not included in the fit because it is contaminated by measurement noise. (b) Stretching exponent for the time-decay of the dynamic structure factor,  $S(\mathbf{k}, t)$ , showing Rouse-dynamics at large  $k$  and Zimm-dynamics at small  $k$ . (c)  $C(\mathbf{r}, \mathbf{r}, \tau = 13.5 \text{ ms})/C(\mathbf{r}, \mathbf{r}, \delta t)$  showing the annular decay pattern of the spatially resolved autocorrelation. The speckled pattern at large  $r$  is due to noise. Scale bar  $2 \mu\text{m}$ . (d) Radial dependence of the correlation time of  $C(\mathbf{r}, \mathbf{r}, \tau)$  (circles), and results of simulated Rouse dynamics (line) [9].

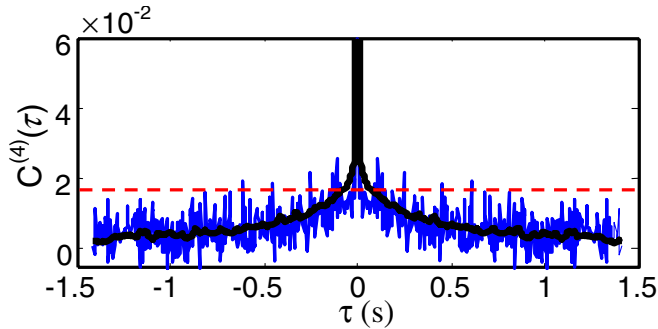


FIG. 5 (color online). Non-Markovian diffusion of the c.m. Plotted are the autocorrelation of the squared step size (blue jagged line); autocorrelation one would expect if the DNA were approximated by a sphere of fluctuating radius, where the radius  $R_G(t)$  is extracted from the images (black bold line); estimate from Ref. [17] for the  $\lim_{\tau \rightarrow 0} C^{(4)}(\tau)$  (red dashed line).

cause non-Markovian diffusion of the c.m. [17], but surmised that this effect would be difficult to observe. This effect arises because  $D$  depends on the instantaneous conformation: more extended conformations diffuse more slowly than more compact conformations. If one examines the diffusion on a time scale short compared to the slowest internal relaxation, the magnitudes (but not directions) of successive Brownian displacements should be correlated.

Fluctuations in  $D$  should lead to a nonzero value of the 4th order correlation function of the pseudofree trajectory:

$$C^{(4)}(\tau) = \text{corr}(\Delta x(t + \tau)^2, \Delta x(t)^2), \quad (5)$$

where  $\Delta x(t) \equiv x(t + \delta t) - x(t)$  is the Brownian hop along the  $x$  axis in the interframe interval,  $\delta t$  (Fig. 5). In the last line of the appendix of Ref. [17], Dubois-Violette and de Gennes predicted that in the limit of strong internal hydrodynamic interactions,  $\lim_{\tau \rightarrow 0} C^{(4)}(\tau) = 1.7\%$ . Averaging  $C^{(4)}(\tau)$  for the 100 ms subsequent to the  $\tau = 0$  spike, we found  $C^{(4)}(\tau) = 1.4\% \pm 0.4\%$  (mean  $\pm$  standard deviation;  $n = 20$  data points), consistent with the prediction of Ref. [17]. Furthermore, we compared the observed shape of  $C^{(4)}(\tau)$  to what one would expect for Brownian diffusion of a sphere with a time-dependent radius,  $R(t)$ , where  $R(t)$  was set equal to the time-dependent radius of gyration,  $R_G(t)$ , which was in turn extracted from the video images (solid black line in Fig. 5). As Fig. 5 shows, this “spherical cow” approximation is in good agreement with the data, validating the hypothesis that the fluctuations in  $D$  arise from internal conformational fluctuations which change the radius of gyration.

For the first time we have measured the spatially resolved density-density correlations of individual molecules of ds  $\lambda$  DNA. The fluctuations show clear signs of hydrodynamic coupling; an effect that was not detected in previous measurements on DNA due to the limited observation time. The fluctuations show as-yet poorly under-

stood radial structure that is averaged away in classical scattering measurements. The diffusion of the c.m. is modulated by the internal fluctuations in the radius of gyration; an effect neglected in the mean-field Zimm picture. The walls of the trap probably perturb the observed dynamics, leading to weaker hydrodynamic couplings than would be occur in free solution. It will be interesting to see how the descriptive statistics presented here change when a trapped molecule of DNA is subjected to physical and chemical perturbations, such as changes in pH, temperature, ionic strength, or the addition of proteins that interact with DNA.

We thank Kit Werley, Joel E. Cohen, and John Brauman for helpful comments. This work was supported in part by NSF Grant No. CHE-0554681 and NIH Grant No. 1R21-RR023149.

\*Electronic address: acohen@post.harvard.edu

- [1] M. Doi and S.F. Edwards, *The Theory of Polymer Dynamics* (Oxford University Press, Oxford, 1988).
- [2] B. J. Berne and R. Pecora, *Dynamic Light Scattering: With Applications to Chemistry, Biology, and Physics* (Dover, New York, 2000).
- [3] K. Kroy and E. Frey, Phys. Rev. E **55**, 3092 (1997).
- [4] D. Lumma, S. Keller, T. Vilgis, and J.O. Radler, Phys. Rev. Lett. **90**, 218301 (2003).
- [5] S. A. Tatarkova and D. A. Berk, Phys. Rev. E **71**, 041913 (2005).
- [6] R. Shusterman, S. Alon, T. Gavrinov, and O. Krichevsky, Phys. Rev. Lett. **92**, 048303 (2004).
- [7] R.M. Robertson, S. Laib, and D.E. Smith, Proc. Natl. Acad. Sci. U.S.A. **103**, 7310 (2006).
- [8] A.E. Cohen and W.E. Moerner, Proc. Natl. Acad. Sci. U.S.A. **103**, 4362 (2006).
- [9] See EPAPS Document No. E-PRLTAO-98-007711 for supplementary text and calculations clarifying some technical issues associated with trapping DNA in the ABEL trap. For more information on EPAPS, see <http://www.aip.org/pubservs/epaps.html>.
- [10] J.-L. Viovy, Rev. Mod. Phys. **72**, 813 (2000).
- [11] B.M. Olivera, P. Baine, and N. Davidson, Biopolymers **2**, 245 (1964).
- [12] A.E. Cohen and W.E. Moerner, Proc. SPIE Int. Soc. Opt. Eng. **5930**, 191 (2005).
- [13] F. Brochard and P.G. de Gennes, J. Chem. Phys. **67**, 52 (1977).
- [14] H. Yamakawa, *Modern Theory of Polymer Solutions* (Harper and Row, New York, 1971).
- [15] M.E. Fisher, J. Chem. Phys. **44**, 616 (1966).
- [16] P. de Gennes, Physics (Long Island City, N.Y.) **3**, 37 (1967).
- [17] E. Dubois-Violette and P. de Gennes, Physics (Long Island City, N.Y.) **3**, 181 (1967).
- [18] Y.-L. Chen, M. D. Graham, J. J. dePablo, G. C. Randall, M. Gupta, and P. S. Doyle, Phys. Rev. E **70**, 060901(R) (2004).